Available online at www.sciencedirect.com

SciVerse ScienceDirect

Energy Procedia 28 (2012) 134 – 139

Energy Procedia

Fuel Cells 2012 Science & Technology – A Grove Fuel Cell Event

The impact on PEMFC of bionic flow field with a different branch

Tao Chen*, Yong Xiao, Tiezhu Chen

School of Mechanical and Electronic Engineering, Wuhan University of Technology, Wuhan 430070, China

Abstract

The branching structure such as tree leaves, animal lungs and so on is universal and unique in nature. These structures are considered to be an optimal network channel for mass transfer and heat transfer. The mass transfer and heat transfer feature of bipolar plates in a proton exchange membrane fuel cell (PEMFC) is similar to them. In our research, the bionic similarity theory is used to design bionic flow fields for bipolar plates in PEMFCs based on leaf venation. It is demonstrated by numerical simulation that the PEMFC performance will be impacted by the number and location of branches in bionic flow fields. The location of branches has a greater impact on the exit velocity; the more branches there are, the more favourable is the discharge of water. Finally, different operating parameters (temperature, pressure, relative humidity, and stoichiometry) in bionic flow fields are chosen to study the PEMFC performance. In this way a kind of excellent flow field structure of bipolar plates in PEMFCs can be achieved.

Keywords: Proton exchange membrane fuel cell (PEMFC); Flow field; Bionics; Leaf venation; Performance

1. Introduction

With the merits of high energy density, fast startup, and longevity, the PEMFC is the most prospective among low-temperature fuel cells. The flow field design of a bipolar plate heavily influences the performance of a PEMFC. It must uniformly distribute the reactant gases over the membrane electrode assembly (MEA) and prevent product water flooding. If either of these functions is impaired by reactants being inefficiently supplied across the MEA, it causes a loss in performance. Additionally, it must provide good electrical contact with the MEA to give a low cell electrical resistance (which in turn will impact the distribution of reactants). The leaves found in nature are considered a natural optimisation of the enhanced

* Corresponding author. Tel: +86-27-87651793; fax: +86-27-87651793.
E-mail address: chent29@whut.edu.cn

1876-6102 © 2012 Published by Elsevier Ltd. Selection and/or peer-review under responsibility of the Grove Steering Committee.
Open access under CC BY-NC-ND license. doi:10.1016/j.egypro.2012.08.047

heat transfer and mass transfer of flow channels. They have a uniform distribution of microtubules, and facilitate the energy and material delivery. The mass transfer and heat transfer of a PEMFC bipolar plate is similar to leaves. The flow field distribution in a PEMFC bipolar plate can be regarded as a self-growth process like leaf vein formation, thus the flow field is started from a given 'seed' and is grown, branched off or degenerated according to a certain growing rule, to form the optimal distribution patterns.

Some researchers have begun to investigate flow field designs with inspirations from nature [1–5]. These bionic flow field designs have demonstrated advantages in distributing reactants and enhancing performance. Kloess et al. [1] combined serpentine and interdigitated patterns with a leaf/lung layout to design a bio-inspired flow layout. They reported that these new designs improved pressure distribution, decreased pressure loss, and increased power density as compared to pure serpentine and interdigitated designs. Chapman et al. [2] claimed that their biomimetic designs enhanced the performance of PEM fuel cells by 16%. They stated that their designs comprised main and sub-feed channels and that tapered, nonlinear channels could improve performance. In Reference [5], a new bipolar plate design inspired by the existing biological fluid flow patterns in a leaf is presented and analysed. The main design criteria in this research are based on more uniform velocity distribution and more homogeneous molar spreading of species along the flow channels, and also higher voltage and power density output at different current densities. By developing a numerical code it was found that the velocity and pressure profiles on the catalyst surface are much more uniform, the reactant concentration on the catalyst surface is much more homogeneous, and the power density is higher than parallel and serpentine flow channels by up to 56% and 26% respectively. The above studies have shown the potential benefits of incorporating natural structures into flow field designs. In this paper, the performance of a PEMFC influenced by the number and location of the bionic flow channel branches will be studied.

2. Mathematical model

Taking the flow field pattern of a PEMFC as the growth process, the designer expects the flow field performance of the fuel cell to show a good growth state under different conditions like leaves. They then constitute a flow field pattern based on the vein growth state through biomimetic analogy theory, to achieve the optimal structure of a fuel cell. In order to calculate conveniently, the primary vein and secondary veins can be simplified and designed to be a main channel with a regular rectangular cross-section, while the net veins can be developed to be sub-flow channels that parallel the primary vein, as shown in Fig. 1.

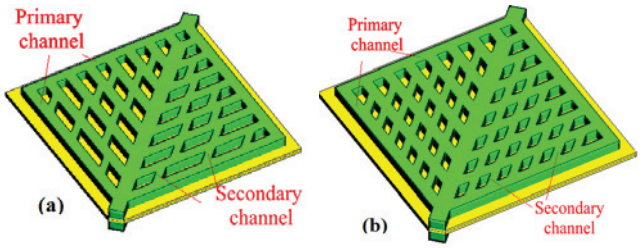

Fig. 1. Flow field patterns.

The internal model of a PEMFC is a complicated model, with heat, fluid and electric fields coupled together. The various factors within the fuel cell interact with each other and restrict each other. The basic equation, which includes the mass conservation equation, mass transfer equation, momentum conservation equation, energy conversation equation, species conservation equation, and current conservation equation, is the foundation of numerical simulation:

$$\nabla.(\varepsilon(\vec{u})) = S_m \quad (1)$$

$$\nabla.(\varepsilon(\vec{u}C_k)) = -\nabla.J_k + S_k \quad (2)$$

$$\nabla.(\varepsilon(\vec{u}\vec{u})) = -\varepsilon\nabla p + \nabla.(\varphi(\nabla\vec{u})) + S_u \quad (3)$$

$$\frac{\partial(\varepsilon\varepsilon\rho_p T)}{\partial t} + \nabla.(\varepsilon(\varepsilon_p \vec{u} T)) = \nabla.(k^{eff}\nabla T) + S_Q \quad (4)$$

$$\frac{\partial(\varepsilon\varepsilon_k)}{\partial t} + \nabla.(\varepsilon(_k \vec{u})) = \nabla.(D_k{}^{eff}\nabla c_k) + S_k \quad (5)$$

$$\nabla.(\sigma_e\nabla\varphi_e) + S_e = 0 \quad \nabla.(\sigma_m\nabla\varphi_m) + S_m = 0 \quad (6)$$

Here ε is porosity, ρ is density, $\vec{u}$ is the velocity vector, S_m is the source item of the mass, C_k is species concentration of species k, J_k is the diffusion flux of species k, S_k is the source item of mass changes, μ is viscosity; S_u is the momentum source item; C_p is specific heat at constant pressure, T is temperature; S_Q is the energy source item, S_k is the source item of species, p is pressure; k^{eff} is the effective thermal conductivity coefficient, D_k^{eff} is effective diffusion coefficient of species, Φ_e and Φ_m are solid phase potential and membrane phase potential, respectively, and σ is conductivity.

3. Solving

3.1 Operating parameter

The side length of the model is 20 mm × 20 mm. The thicknesses of the diffusion layer, catalyst layer, and proton exchange membrane are 0.2 mm, 0.015 mm and 0.03 mm, respectively. The dimension of the primary channel width and height is 1 mm. The operating temperature is 353K (80°C), operating pressure is 1 atm, open voltage is 1.17 V. The other parameters are shown in Table 1.

Table 1. Operating parameters.

Parameters	Value
Anode reference current density (A m^{-3})	1.5×10^9
Cathode reference current density (A m^{-3})	1×10^5
Hydrogen diffusion coefficient (m^2 s^{-1})	3.5×10^{-5}
Oxygen diffusion coefficient (m^2 s^{-1})	5×10^{-5}
Vapor diffusion coefficient (m^2 s^{-1})	8×10^{-5}
Diffusion coefficient of other species (m^2 s^{-1})	3×10^{-5}
Porosity of diffusion layer	0.5
Viscosity coefficient of diffusion layer (m^{-2})	1×10^{12}
Catalyst layer surface to volume ratio (m^{-1})	2×10^5
Conduction coefficient of layer	1
Conduction exponent of layer	1
Contact resistivity (ohm m^2)	2×10^{-6}
Catalyst layer Cp (J/kg K)	710
Diffusion layer thermal conductivity (W/m K)	1.6

3.2 Supply of reaction gas

The reactant supply of the anode and cathode are:

$$\dot{m}_a = \frac{RT_0}{P_a - RH_a P_{sat}} \frac{\rho_a \xi_a I_{ref} A}{2F} \tag{7}$$

$$\dot{m}_c = \frac{RT_0}{P_c - RH_c P_{sat}} \frac{\rho_c \xi_c I_{ref} A}{4F} \tag{8}$$

Within the equations, R is the gas constant, T_0 = 353K, P is the operating pressure, RH the relative humidity, P_{sat} the local saturated vapour pressure, ρ the density of the reaction gas, ξ the stoichiometric ratio, I_{ref} the reference current density, A the active area, and F the Faraday constant. After assigning value for these variables in the equations, we can figure out that the mass fluxes required in the anode and the cathode are 3.293×10^{-6} kg s^{-1} and 2.857×10^{-7} kg s^{-1}, respectively.

3.3. Boundary conditions and solving

The PEM module of Fluent software was used to solve the model. According to the configuration method in Fluent, the mass flux, species concentration of fuel, and inlet temperature at the inlet must be set. At the outlet, the pressure outlet was set as the boundary conditions. For a fixed wall, the species flux is zero. Temperature was assumed to be constant. The calculation process first discretises the coupled and nonlinear equation with the finite volume method, and then uses the SIMPLE algorithm to iterate.

4. Results and analysis

The polarisation curves of the two flow field patterns are shown in Fig. 2. It can be seen from the Figure that with the increase in current density the voltage declines gradually because of a variety of polarisation phenomena inside the fuel cells. Differences in structure play a minor role in the current density when the operating voltage is above 0.8 V, but it plays a bigger role when the operating voltage is lower than 0.7 V, which is particularly apparent when the current density is high. Under the same operating voltage, flow field (b) has a higher current density, about 2.6% higher than flow field (a). The maximum power density of (b) is 3.3% higher than (a). Therefore a reasonable flow pattern is conducive to the improvement in fuel cell performance.

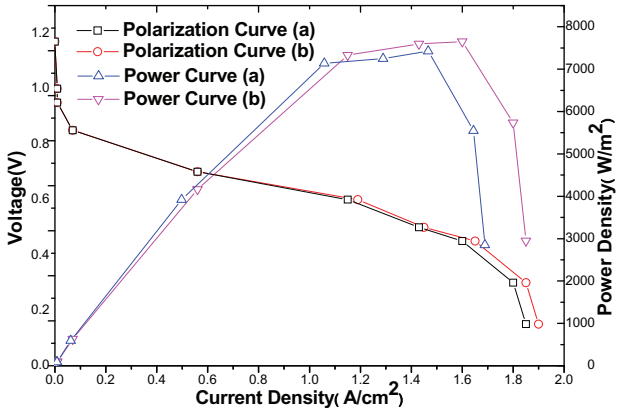

Fig. 2. I-V curves.

Fig. 3 shows the water content distribution of the diffusion layer and catalyst layer interface (GDL/cat). It can be seen from the Figure that there is less water near the inlet, while a large amount of water gathers below the bipolar plates near the outlet, mainly due to the larger air current that brings the byproduct water to the outlet. It can also be seen from Fig. 3 that there is less water in the flow channels, while a large amount of water gathers below the bipolar plates. The reason is that the rib is in close contact with the diffusion layer, making it difficult to get enough reaction gas; then byproduct water gathers under the rib. Consequently, the gas diffusivity has an effect on the fuel cell performance. In Fig. 3 the average water content of (a) is larger than that of (b) when inputting the same amount of gas.

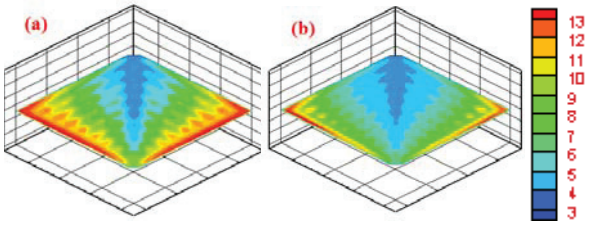

Fig. 3. Contours of water content at the surface of GDL/cat.

Fig. 4 shows the contour of streamlines near the inlet. The near-wall and middle part of reaction gas in (a) form a vortex, which is not conducive to water discharge. In Fig. 4(b), the reactant performs good fluid dynamics, and heat can be brought away promptly. This suggests that the earlier the flow channel branches and the larger the number of branch flow channels, the smoother the streamline distribution will be and the more conducive to the exchange of reaction gas between adjacent main channels. Comparing with conventional flow field patterns, the existence of secondary channels reinforces flow between adjacent flow channels and increases the number of flow channels, bringing the formation of diversion and confluence of flow between units of biomimetic structure, and then causing visible velocity changes, airflow disruptions and pressure changes, leading to more reaction gas participating in the electrochemical reaction, which is conducive to the improvement of fuel cell performance.

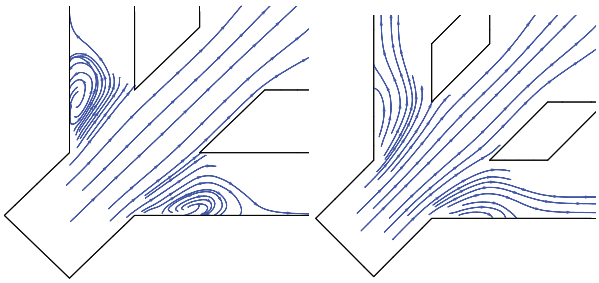

(a) (b)

Fig. 4. Contours of streamlines at the inlet.

Fig. 5 shows the mole concentration distribution of oxygen in the diffusion layer – the catalyst layer (GDL/cat) of the above-mentioned (a) and (b) patterns. It can be seen from the Figure that the mole concentration of oxygen gradually reduces, mainly because as the electrochemical reaction proceeds, oxygen is consumed by degrees. By comparing the aforementioned two flow fields, we find that the oxygen mole concentration is symmetric along the main flow channel direction; the closer the flow channel is to the primary channel, the higher the mole concentration of oxygen, and the mole fraction of oxygen at the end of the primary channel is almost zero. Flow field pattern (b) has a more even oxygen

mole concentration distribution, which is beneficial to the uniform conduct of the electrochemical reaction, and has a significant impact on the even distribution of current density.

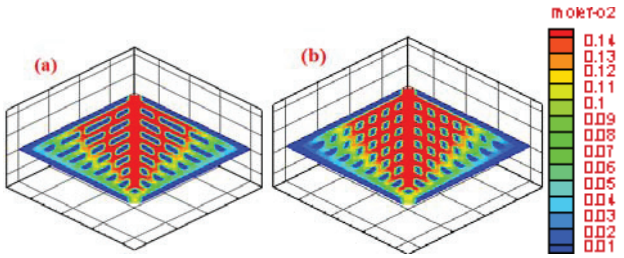

Fig. 5. Contours of oxygen molar concentration at the surface of GDL/cat.

5. Conclusions

The following conclusions can be drawn from the numerical simulation of newly designed flow field patterns based on plant veins:

(1) When operating voltage is lower than 0.7 V, differences in flow field patterns have greater impact on the current density, which is especially apparent at high current density.

(2) There is less water near the inlet, but a large amount of water near the outlet. Water content under the flow channels is low, but it is high under bipolar plates.

(3) The oxygen mole concentration is symmetric along the main flow channel. The closer the flow channel is to the primary channel, the higher the mole concentration of oxygen. The mole fraction of oxygen at the end of the primary channel is almost zero.

(4) Because of the existence of secondary channels in the new biomimetic flow field, the adjacent primary channels can form diversion and confluence of flow, causing visible velocity changes, airflow disruptions and pressure changes and leading to more reaction gas participating in the electrochemical reaction, which is conducive to the improvement in fuel cell performance.

(5) The new biomimetic flow field patterns, compared with traditional parallel flow fields, possess more uniform gas distribution, a higher gas consumption ratio, generate less ohmic heat, and take the effect of structure on the manufacturing cost into consideration.

Acknowledgments

The authors would like to thank the National Science Foundation of China (Grant Number: 50975214) and the Wuhan Science & Technology Bureau (Grant Number: 201010621229) for funding this study.

References

[1] J.P. Kloess, X. Wang, J. Liu, Z. Shi, L. Guessous, Investigation of bio-inspired flow channel designs for bipolar plates in proton exchange membrane fuel cells, *J. Power Sources* 2009; **188**: 132–140.

[2] A. Chapman, I. Mellor, Development of Biomimetic™ flow field plates for PEM fuel cells. Eighth Grove Fuel Cell Symposium, London, UK, 24–26 September 2003.

[3] C. Damian-Ascencio, A. Hernandez-Guerrero, F. Ascencio-Cendejas, Entropy generation analysis for a PEM fuel-cell with a biomimetic flow field. ASME 2009 International Mechanical Engineering Congress and Exposition, Florida, 2009.

[4] S. Kjelstrup, M.O. Coppens, J.G. Pharoah, P. Pfeifer, Nature inspired energy and material efficient design of a polymer electrolyte membrane fuel cell, *Energy & Fuels* 2010; **24**: 5097–5108.

[5] R. Roshandel, F. Arbabi, G.K. Moghaddam, Simulation of an innovative flow-field design based on a bio inspired pattern for PEM fuel cells, *Renewable Energy* 2012, **41**: 86–95.